

## Stability of graphene band structures against an external periodic perturbation: Na on graphene

C. G. Hwang,<sup>1,4</sup> S. Y. Shin,<sup>1</sup> Seon-Myeong Choi,<sup>1</sup> N. D. Kim,<sup>1,5</sup> S. H. Uhm,<sup>1</sup> H. S. Kim,<sup>1</sup> C. C. Hwang,<sup>2</sup> D. Y. Noh,<sup>3</sup> Seung-Hoon Jhi,<sup>1</sup> and J. W. Chung<sup>1,\*</sup><sup>1</sup>Department of Physics, Pohang University of Science and Technology, 790-784 Pohang, Korea<sup>2</sup>Beamline Research Division, Pohang Accelerator Laboratory (PAL), 790-784 Pohang, Korea<sup>3</sup>Department of Materials Science and Engineering, Gwangju Institute of Science and Technology, 500-712 Gwangju, Korea<sup>4</sup>Materials Sciences Division, Lawrence Berkeley National Laboratory, Berkeley, California 94720, USA<sup>5</sup>Department of Physics, Columbia University, New York, New York 10027, USA

(Received 26 November 2008; revised manuscript received 2 February 2009; published 27 March 2009)

The electronic structure of Na-adsorbed graphenes formed on the 6H-SiC(0001) substrate was studied using angle-resolved photoemission spectroscopy with synchrotron photons and *ab initio* pseudopotential calculations. It was found that the band of the graphenes sensitively changes upon Na adsorption especially at low temperature. With increasing Na dose, the  $\pi$  band appears to be quickly diffused into the background at 85 K whereas it becomes significantly enhanced with its spectral intensity at room temperature (RT). A new parabolic band centered at  $k \sim 1.15 \text{ \AA}^{-1}$  also forms near Fermi energy with Na at 85 K while no such band was observed at RT. Such changes in the band structure are found to be reversible with temperature. The changes in the  $\pi$  band of graphene are mainly driven by the Na-induced potential especially at low temperature where the potential becomes periodic due to the crystallized Na overlayer. The new parabolic band turns out to be the  $\pi$  band of the underlying buffer layer partially filled by the charge transfer from Na adatoms. The increase in the hopping rate of Na adatoms at RT by 5 orders of magnitude prevents such a charge transfer, explaining the absence of the new band at RT.

DOI: [10.1103/PhysRevB.79.115439](https://doi.org/10.1103/PhysRevB.79.115439)

PACS number(s): 73.21.-b, 73.22.-f, 71.10.Pm, 73.20.At

## I. INTRODUCTION

Recent spur on the study of graphene has been motivated mostly by the unusual nature of its effectively massless charge carriers, so-called Dirac fermions, leading to some exotic electronic properties. Its potential application for future nanometer-scale devices, on the other hand, has also been under extensive exploration. Graphene is a flat atomic single layer of graphite having a hexagonal crystalline symmetry with two atoms per unit cell. Its low energy band structure shows the almost linear  $\pi$  bands with a vanishing density of states at the Dirac point of charge neutrality where the valence band ( $\pi$  band) and conduction band ( $\pi^*$ ) meet at the  $K$  point of the hexagonal Brillouin zone. With increasing reports on the electronic properties of graphene layers including the anomalous quantum Hall effects,<sup>1-3</sup> the possibility of utilizing such features for atomic-scale devices seems to increase as seen also in the bilayer graphene.<sup>4</sup> Ohta *et al.*<sup>4</sup> showed that the adsorption of potassium on bilayer graphene modifies the potential symmetry in the graphene layers resulting in the change in energy gap at the  $K$  point. This provides a way of controlling the conductivity of the charge carriers for the switching capability in the atomic scale. Moreover, recent calculations also provide a way to control the electrical properties of graphene by utilizing the chiral nature of the Dirac fermions of graphene.<sup>5</sup> Park *et al.*<sup>5</sup> showed that the Dirac fermions of graphene are sensitive to external potentials so as to show, for example, the anisotropic renormalization of group velocity at the  $K$  point. Such features can be more drastic when external potentials have a periodicity ( $L$ ) comparable to the graphene lattice constant ( $a_0 \sim 2.46 \text{ \AA}$ ). In addition, the lifetime of Dirac fermions is significantly reduced when  $L \leq a_0$  due to the enhanced back-

scattering between states with momentums of  $+k$  and  $-k$ .<sup>6,7</sup> There have been several studies using angle-resolved photoemission spectroscopy (ARPES),<sup>8-10</sup> but it has not been comprehensively understood yet how external perturbations at such length scales affect the electronic structure of graphenes. It will be interesting to study the stability of graphene electronic structures against foreign perturbations especially when their range is comparable to the graphene lattice constant.

We report here an example of such a study wherein the presence of an external potential on graphene significantly affects the nature of Dirac fermions not only by the periodicity of the potential but also more remarkably by the degree of order of the potential especially when  $L \sim a_0$ . We have investigated the behavior of the  $\pi$  band along the  $\Gamma$ - $K$  direction as we adsorb Na on graphene at two different temperatures, 85 K and room temperature (RT). We find remarkable changes in the  $\pi$  band as a function of Na dose at both temperatures. We also notice the appearance of a parabolic band centered at  $k = 1.15 \text{ \AA}^{-1}$  only at 85 K. Furthermore, the  $\pi$  band exhibits quite a different behavior with Na on a bilayer graphene from that of a single layer graphene. We mainly discuss such changes in the  $\pi$  band of graphene in terms of the variation in the induced potential by Na adsorption. We also discuss the origin and characteristics of the new parabolic band from our band calculation.

## II. METHODS

We have obtained our ARPES data by using the ARPES chamber at the beamline 3A2 of the Pohang Accelerator Laboratory in Korea using synchrotron photons of energy at 34 eV. The chamber was equipped with a hemispherical Sci-

enta R4000 electron analyzer which provides an overall energy resolution of 113 meV. All measurements were made with the chamber under  $1 \times 10^{-10}$  Torr. An *n*-type 6H-SiC(0001) substrate was pretreated by annealing at 900 °C under the Si flux generated from a resistively heated Si wafer at 1150 °C to obtain the  $\sqrt{3} \times \sqrt{3}R30^\circ$  phase. We then continued to anneal the substrate further to obtain a carbon-rich surface with the  $6\sqrt{3} \times 6\sqrt{3}$  phase as reported earlier.<sup>11</sup> Single layer and bilayer graphenes were self-assembled when this precursor phase was annealed for an extended time period. We have used a commercial (SAES) getter source to deposit Na on the graphene surface. Because of the three possible structural phases usually coexisting on the graphene layers formed on the SiC(0001) surface,<sup>12</sup> it would be quite hard, if not impossible, to determine the absolute coverage of Na adatoms. We thus measured work function change to estimate Na coverage.

In order to interpret our band data, we have also performed *ab initio* pseudopotential total-energy calculations with a plane-wave basis set.<sup>13</sup> The exchange correlation of electrons was treated within the generalized gradient approximation as implemented by Perdew-Berke-Ernzerhof.<sup>14</sup> The cutoff energy for the expansion of wave functions and potentials in the plane-wave basis was chosen to be 400 eV, and the Brillouin zone sampling was done with the Monkhorst-Pack special *k*-point method with a grid of  $5 \times 5 \times 1$  for the  $\sqrt{3} \times \sqrt{3}R30^\circ$  buffer-layer phase. We used the projector augmented wave pseudopotentials as provided by the software package (Vienna *ab initio* simulation package).<sup>15</sup> The atomic relaxation was carried out until the Hellmann-Feynman forces were less than 0.02 eV/Å. The vacuum layer in the supercell used in our calculations is set to be 8 Å, which is enough to minimize the artificial inter-layer interaction.

### III. RESULTS AND DISCUSSIONS

The phase of single layer graphene formed on the SiC(0001) surface was first indicated by its characteristic low-energy electron diffraction (LEED) spots as seen in Fig. 1(a). We also find from their unique LEED spots that the surface contains not only the  $1 \times 1$  phase of single layer graphene but also the  $6\sqrt{3} \times 6\sqrt{3}R30^\circ$  phase of the exposed buffer layer. A primary electron energy of 98 eV is used to monitor the changes in the LEED pattern during the preparation process. The electronic structure of the graphene thus prepared has been measured using ARPES along the  $\Gamma$ -*K*-*M* direction of graphene. Photoelectron intensity map near the zone boundary *K* shows the well-known graphene  $\pi$  band [Fig. 1(b)], indicative of a single layer graphene. This linear dispersion of the  $\pi$  band suggests that the charge carriers in graphene can be considered as massless Dirac fermions. The single layer graphene suggested by LEED, however, has been finally confirmed by observing the unsplit linear  $\pi$  band along the  $\Gamma$ -*K*-*M* direction as shown in Fig. 1(b) before developing into the split  $\pi$  band with further annealing due to the formation of multiple graphene layers.<sup>4</sup> Here we observe only one band rather than the two forming a conical shape  $\pi$  band due to the chiral property of graphene.<sup>16,17</sup> From the

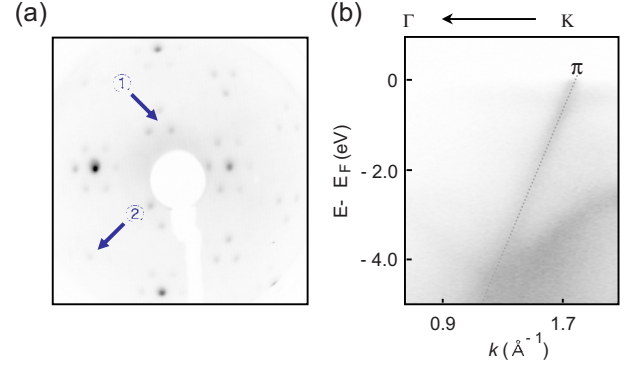


FIG. 1. (Color online) (a) A typical LEED pattern from a single layer graphene formed on SiC substrate measured with a primary beam energy of 98 eV. The characteristic LEED spots of the  $6\sqrt{3} \times 6\sqrt{3}R30^\circ$  buffer layer appear as three spots forming a triangle around the point marked by arrow 1 together with those hexagonal satellite spots around normal spots. The spots unique to the  $1 \times 1$  phase of the single graphene layer are indicated by arrow 2. (b) The formation of a single layer graphene is finally confirmed by observing the unsplit linear  $\pi$  band of graphene in the ARPES intensity map near the *K* point ( $k=1.7 \text{ \AA}^{-1}$ ). The band was measured with synchrotron photons of energy 34 eV along the  $\Gamma$ -*K*-*M* direction.

slope of the band we estimate the Fermi velocity  $v_F=1.1 \pm 0.074 \times 10^6$  m/s to be in good agreement with an earlier value of  $10^6$  m/s from Shubnikov-de Haas oscillations<sup>18</sup> where the effective carrier mass of graphene was estimated to be about  $0.02 \sim 0.07 m_0$  with  $m_0$  being the free-electron mass.<sup>18</sup>

In Fig. 2, we show progressive changes in the  $\pi$  band with increasing function of Na dose on single layer [Figs. 2(a)–2(e)] and bilayer [Figs. 2(f)–2(j)] graphenes at temperature of 85 K. The amount of Na atoms adsorbed is indicated by work function change ( $\Delta\phi$ ) induced by Na adsorption. As a guide, we estimate the coverage of Na at  $\Delta\phi=-0.36$  eV as  $\frac{1}{4}$  monolayers considering the saturation value of  $\Delta\phi_m=-1.4$  eV for the Na-added graphite.<sup>19</sup> The linewidth of the  $\pi$  band in Fig. 2(f) appears to be much broader than that in Fig. 2(a) of the single layer graphene. Although our resolution does not resolve the broadened band into two or more split bands, the measured linewidth of  $0.08 \pm 0.02 \text{ \AA}^{-1}$  indicates the  $\pi$  band from a bilayer graphene.<sup>4</sup> From Figs. 2(a)–2(e), one immediately notices that the adsorption of Na on the single layer graphene quickly deteriorates the  $\pi$  band by significantly weakening its spectral intensity as well as broadening the linewidth and concomitantly accompanies a new parabolic band near Fermi energy. The deterioration of the  $\pi$  band becomes worse while the parabolic band becomes stronger with increasing Na coverage. The corresponding changes induced by Na adsorption on the bilayer graphene in Figs. 2(f)–2(j) are quite different from those on the single layer graphene; the  $\pi$  band remains strong in intensity while slightly broadening with increasing Na dose. The parabolic band is still there but becomes much weaker compared to the one from the single layer graphene at the same dose of Na.

We first investigate the nature of the parabolic band. Figure 3 shows this new band at  $\Delta\phi=0.30$  eV. The red circles in Fig. 3(a) denote the maxima in spectral intensity obtained

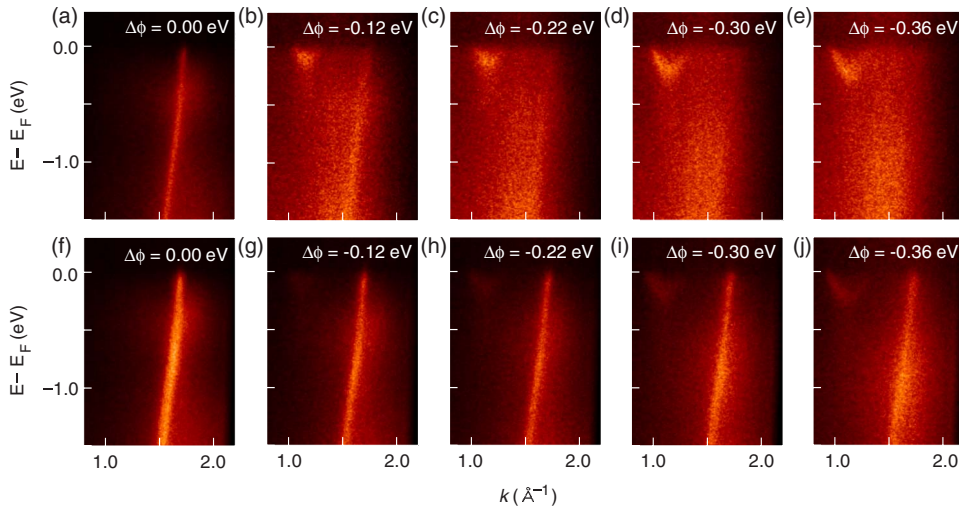


FIG. 2. (Color online) (a)–(e) The progressive change in the band structure of a single layer graphene along the  $\Gamma$ - $K$ - $M$  direction as a function of Na dose at 85 K. With increasing Na dose, the linear  $\pi$  band quickly deteriorates both in intensity and in linewidth while a new parabolic band develops. (f)–(j) Corresponding changes for a bilayer graphene at 85 K.

by fitting the EDCs with a Lorentzian function for  $0.98 \leq k \leq 1.32 \text{ \AA}^{-1}$  [see Fig. 3(c)]. The dispersion of the new band obtained from the momentum distribution curve at Fermi energy in Fig. 3(b) appears to be parabolic with a minimum at  $k \sim 1.15 \text{ \AA}^{-1}$  for  $E_m = 0.19 \text{ eV}$  below the Fermi level. We obtain charge carrier mass  $m = 0.58 \pm 0.07 m_0$ , which is 8.3  $\sim$  29 times heavier than that of the Dirac electrons of the clean graphene without Na.

Interestingly, the  $\pi$  band quickly fades away with the development of the new band as Na dose increases on the single layer graphene, which is more apparent in Fig. 4(a) where the MDCs change with Na dose. The  $\pi$  band almost disappears while the spectral intensity of the new band is enhanced, showing the two peaks marked by arrows of the parabolic band centered at around  $1.15 \text{ \AA}^{-1}$ . The  $\pi$  band, however, behaves quite differently with Na for the bilayer

graphene mostly maintaining its intensity as seen in Fig. 4(b). The rapid quenching of the  $\pi$  band of the single layer graphene reflects a destructive effect associated with the Na adatoms on the top graphene layer. The sustaining intensity of the  $\pi$  band in the bilayer graphene in Figs. 2(f)–2(j) comes from the second layer graphene, which is not affected by Na adsorption. The inset of Fig. 4(b) shows the change in linewidth as a function of Na dose. The linewidth initially decreases down to the value of a single layer graphene and then begins to increase with further dose of Na, which supports this interpretation.

We also performed *ab initio* pseudopotential total-energy calculations. Figure 5 shows the plausible binding site of Na atoms on the  $\sqrt{3} \times \sqrt{3} R30^\circ$  buffer layer in Fig. 5(a) and the Brillouin zones of the  $1 \times 1$  of graphene together with those of the buffer layer in Fig. 5(b). With the Na coverage of 0.63 monolayer, the adsorption energy  $E_{ad}$  calculated to be 0.86 eV at the most favorable binding sites is compared to the next favored hollow site of 0.72 eV. All hollow sites of

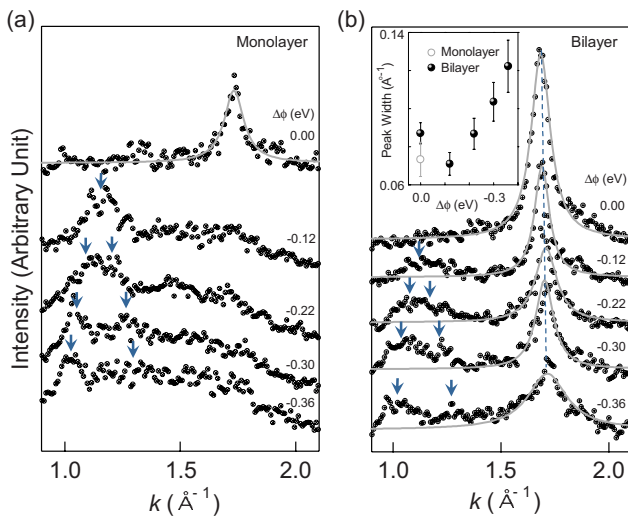


FIG. 3. (Color online) (a) Photoemission intensity map of a new band from a single layer graphene along the  $\Gamma$ - $K$  direction at Na dose of  $\Delta\phi = -0.30$ . (b) The new band appears to be a parabolic shape with a minimum at  $\sim 1.15 \text{ \AA}^{-1}$ , which is apparent in the momentum distribution curve (MDC) at the Fermi level and also in (c) where energy distribution curves (EDCs) are shown between  $k_i = 0.98 \text{ \AA}^{-1}$  and  $k_f = 1.32 \text{ \AA}^{-1}$ . The red circles denote the maxima in intensity.

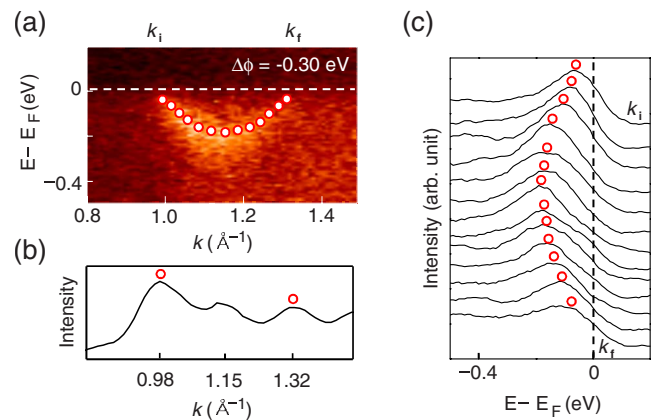


FIG. 4. (Color online) The spectral changes in the MDCs with increasing Na dose measured in terms of  $\Delta\phi$  obtained from (a) single layer graphene and (b) bilayer graphene. The down arrows indicate the intensity maxima of the parabolic new band. The solid gray curves are Lorentzian fit curves of the  $\pi$  band of graphene. The vertical dotted line in (b) shows the shift of the  $\pi$  band toward higher binding energy with increasing Na dose. Inset shows the change in bandwidth with Na adsorption.



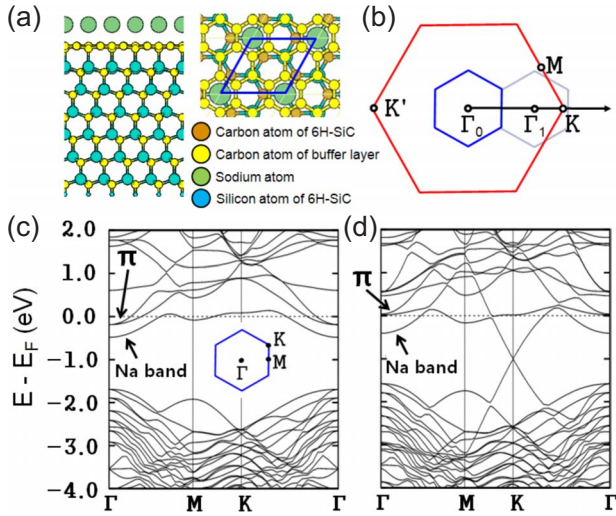


FIG. 5. (Color online) (a) Side (left) and top (right) views of the atomic arrangement for the  $\sqrt{3} \times \sqrt{3}R30^\circ$  buffer layer/6H-SiC assuming Na coverage of 0.63 monolayer. (b) The Brillouin zone of  $1 \times 1$  clean graphene (red hexagon) and that of the  $\sqrt{3} \times \sqrt{3}R30^\circ$  buffer layer (blue hexagon). The shifted Brillouin zone of the  $\sqrt{3} \times \sqrt{3}R30^\circ$  phase shifted by  $1.37 \text{ \AA}^{-1}$  is also shown by pale blue hexagon. Calculated band structures (c) for the  $\sqrt{3} \times \sqrt{3}R30^\circ$  buffer-layer/6H-SiC system and (d) for the single layer graphene/buffer-layer/6H-SiC system. Note that the  $\pi$  bands of the buffer layer near Fermi energy in the vicinity of the  $\Gamma$  point appeared to be partially occupied in (c) for the buffer layer while they are empty in (d) for the graphene layer.

graphene appear to have  $E_{ad}=0.73 \text{ eV}$ . This variation in Na adsorption energy in the buffer layer is attributed to the selective bonding of buffer-layer carbon atoms to the substrate. In contrast, all hollow sites in isolated single layer graphenes were calculated to have the same Na adsorption energy of  $0.73 \text{ eV}$ . The adsorption energy of Na in an isolated single graphene increases to  $1.03 \text{ eV}$  when Na atoms form a single crystalline layer on top of the graphene that corresponds to the (110) plane of bulk Na. At low temperatures, our calculations indicate that Na would readily form islands instead of being well dispersed, which is in fact consistent with the scanning tunneling microscopy measurements of Na islands on graphite.<sup>20</sup> We note that SiC substrates in our measurement are likely to have exposed buffer layers without being covered by either single or bilayer graphenes.<sup>12</sup>

Figure 5 shows our calculated band structures of the buffer layer (without topmost graphene layer) in Fig. 5(c) and the single graphene layer (on top of the buffer) in Fig. 5(d), respectively, with Na adsorbed. One immediately finds the three partially filled bands near the  $\Gamma$  point in Fig. 5(c) originating the upper two from the  $\pi$  electrons in the buffer layer and the lower one from the Na adatoms. Since the buffer-layer  $\pi$  bands are completely empty without Na adatoms,<sup>21</sup> the  $\pi$  bands of the buffer layer are rigidly shifted down by the charge transfer from Na adatoms to the  $\pi$  bands. The nearly empty upper  $\pi$  bands in Fig. 5(d) then indicate that the charge transfer from Na occurs only at the top graphene layer with the underlying buffer layer almost intact. As depicted in Fig. 5(b) since the separation between the  $\Gamma_0$  and the  $\Gamma_1$  of the buffer layer is  $\Delta k=1.37 \text{ \AA}^{-1}$  much

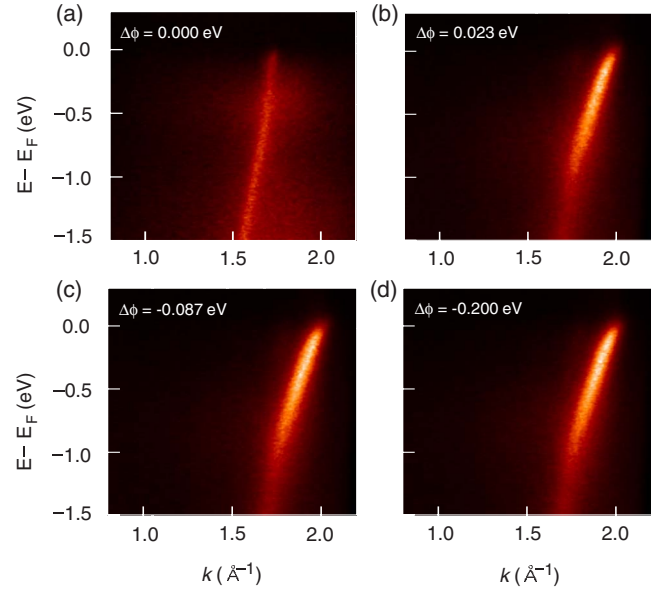


FIG. 6. (Color online) (a)–(d) The corresponding changes as in Figs. 2(a)–2(e) with the sample at RT. The changes are quite different from those in Fig. 2 showing the  $\pi$  band rigidly shifted toward the higher binding energy with enhanced spectral intensity. One also notes the absence of a new parabolic band near Fermi energy in the vicinity of the  $K$  point.

shorter than  $\Delta k=2.10 \text{ \AA}^{-1}$  of the Na (110) plane, the new parabolic band observed in Fig. 2 must be the  $\pi$  bands of the buffer layer partially filled by electrons from Na adatoms. The effective masses of the two buffer-layer  $\pi$  bands are calculated to be  $0.63$  and  $1.35 m_0$ , respectively. We note that the effective mass of the upper one is quite close to the observed value of  $0.58 \pm 0.07 m_0$ . The relatively weak parabolic band seen from the bilayer graphene in Figs. 2(f)–2(j) may be caused by the reduced area of the exposed buffer layer compared to that of the single layer graphene.

Next, we discuss the origin of the deterioration of the  $\pi$  band with Na adsorption. One may think of two plausible causes: (1) due to the random scattering of photoelectrons from the disordered Na adatoms or (2) due to the reduced mean-free path of charge carriers by enhanced backscatterings of charge carriers from Na-induced periodic potentials. The first cause, however, can be easily ruled out by our data in Fig. 6, which shows the corresponding behavior of the  $\pi$  band of the single layer graphene at RT. Here, one immediately notices neither a new parabolic band nor the deterioration of the  $\pi$  band with increasing Na. Instead, the  $\pi$  band becomes stronger in intensity and shifts toward the higher binding energy by about  $0.5 \text{ eV}$ . One also notes that the direction of curvature of the band changed from the one at  $85 \text{ K}$ . Such a change in the curvature has also been observed for the  $K$ -adsorbed graphene.<sup>22</sup> Interestingly, we find that the strong  $\pi$  band at RT begins to deteriorate upon cooling the sample and eventually reproduces the low-temperature features in Fig. 2. The change in the  $\pi$  band of graphene with Na appears to be reversible in temperature. We thus attribute the second cause to the Na-induced weakening of the  $\pi$  band of graphene assuming that Na adatoms form crystalline islands at low temperature giving rise to a certain form of a periodic potential.

If Na crystallizes at 85 K in the form of a layer corresponding to the (110) plane of bulk Na crystal as the Na islands formed on graphite,<sup>20</sup> the periodicity  $L$  of the Na-induced potential may be similar to  $a_0$  of the graphene lattice constant. Such a potential may severely modify the band structure in a way to reduce the mean-free path of charge carriers within graphene by enhanced backscatterings of charge carriers as noted earlier.<sup>5-7,23</sup> The formation of such crystalline Na islands at 85 K is indeed highly likely, considering the significantly reduced hopping rate between the hollow binding sites ( $\nu = \nu_0 e^{-E_d/k_B T}$ , where  $\nu_0$  is an attempt frequency and  $k_B$  is the Boltzmann constant), which is about  $3.65 \times 10^5$  times smaller than that at RT. Here, we have used the diffusion barrier of 0.13 eV between the most stable hollow sites for Na on graphene. The stronger and shifted  $\pi$  band at RT suggests that the  $\pi$  band is shifted down rigidly toward the higher binding energy side revealing the highly occupied band near Fermi level as also observed when  $K$  is absorbed.<sup>22</sup> On the other hand, the increased hopping rate of Na at RT drives the delocalization of charge carriers<sup>24</sup> and reduces the donation of charges to the buffer layer leaving the  $\pi$  band of the buffer layer empty as we observe in Fig. 6. Another interesting question is why the direction of the curvature of the band changes with Na adsorption at RT from that at 85 K. Since the band dispersion along  $K$ - $M$  is different from that along  $\Gamma$ - $K$  and the slope of the band along  $K$ - $M$  is smaller than that along  $\Gamma$ - $K$  according to our calculations (not shown), the  $\pi$  band extended to  $\Gamma$ - $K$ - $M$  is to show a change near the  $K$  point ( $k=1.7 \text{ \AA}^{-1}$ ). Apparently Na adsorption affects differently to the band along  $K$ - $M$  compared to that along  $\Gamma$ - $K$  causing the change in the curvature. As for  $K$  adsorption,<sup>12</sup> such a change might result from many-body

interaction probably enhanced by van Hove singularities.<sup>25</sup>

#### IV. CONCLUSION

By adsorbing Na on graphene at two different temperatures (RT and 85 K) we observe that the band structure of graphene formed on SiC substrate becomes quite sensitively modified by the Na-induced periodic potential especially when the potential becomes periodic with a periodicity comparable to the lattice constant of graphene. The frozen  $\pi$  band of graphene quickly weakens in intensity and broadens its linewidth with Na added at low temperature while it becomes stronger but is rigidly shifted toward the higher binding energy with Na at RT. A new parabolic band observed only at 85 K by adding Na is found to be the  $\pi$  band of the underlying buffer layer partially filled by the charges from Na. Such an extremely sensitive nature of Dirac fermions in graphene to external impurities as well as temperature demands a more careful study of transport properties of graphene for future practical applications in developing graphene-based electronic devices.

#### ACKNOWLEDGMENTS

This work was supported by the Korea Science and Engineering Foundation (KOSEF) funded by the Korea government (MEST) under Grant No. R01-2008-000-20020-0 and also in part by the NCRC under Grant No. R15-2008-006-01001-0. D. Y. Noh acknowledges the support from National Research Laboratory under Program No. M10400000045-04J0000-04510.

\*jwc@postech.ac.kr

- <sup>1</sup>Y. Zhang, Y.-W. Tan, H. L. Stormer, and P. Kim, *Nature (London)* **438**, 201 (2005).
- <sup>2</sup>C. L. Kane and E. J. Mele, *Phys. Rev. Lett.* **95**, 226801 (2005).
- <sup>3</sup>G. Li and E. Y. Andrei, *Nat. Phys.* **3**, 623 (2007).
- <sup>4</sup>T. Ohta, A. Bostwick, J. L. McChesney, T. Seyller, K. Horn, and E. Rotenberg, *Phys. Rev. Lett.* **98**, 206802 (2007).
- <sup>5</sup>C.-H. Park, L. Yang, Y.-W. Son, M. L. Cohen, and S. G. Louie, *Nat. Phys.* **4**, 213 (2008).
- <sup>6</sup>T. Ando and T. Nakanishi, *J. Phys. Soc. Jpn.* **67**, 1704 (1998).
- <sup>7</sup>T. Ando, T. Nakanishi, and R. Saito, *J. Phys. Soc. Jpn.* **67**, 2857 (1998).
- <sup>8</sup>Friedrich Reinert and Stefan Hüfner, *New J. Phys.* **7**, 97 (2005).
- <sup>9</sup>A. Lanzara *et al.*, *Nature (London)* **412**, 510 (2001).
- <sup>10</sup>G.-H. Gweon, T. Sasagawa, S. Y. Zhou, J. Graff, H. Takagi, D.-H. Lee, and A. Lanzara, *Nature (London)* **430**, 187 (2004).
- <sup>11</sup>C. Riedl, A. A. Zakhharov, and U. Starke, *Appl. Phys. Lett.* **93**, 033106 (2008); Wei Chen *et al.*, *Surf. Sci.* **596**, 176 (2005).
- <sup>12</sup>T. Ohta, F. El Gabaly, A. Bostwick, J. McChesney, K. V. Emtsev, A. K. Schmid, T. Seyller, K. Horn, and E. Rotenberg, *New J. Phys.* **10**, 023034 (2008).
- <sup>13</sup>M. L. Cohen, *Phys. Scr.*, T **T1**, 5 (1982).
- <sup>14</sup>J. P. Perdew, K. Burke, and M. Ernzerhof, *Phys. Rev. Lett.* **77**, 3865 (1996).
- <sup>15</sup>G. Kresse and J. Hafner, *Phys. Rev. B* **49**, 14251 (1994).
- <sup>16</sup>E. L. Shirley, L. J. Terminello, A. Santoni, and F. J. Himpsel, *Phys. Rev. B* **51**, 13614 (1995).
- <sup>17</sup>M. Mucha-Kruczyński, O. Tsypliyat'yev, A. Grishin, E. McCann, V. I. Fal'ko, A. Bostwick, and E. Rotenberg, *Phys. Rev. B* **77**, 195403 (2008).
- <sup>18</sup>K. S. Novoselov, A. K. Geim, S. V. Morozov, D. Jian, M. I. Katsnelson, I. V. Grigorieva, S. V. Dubonos, and A. A. Firsov, *Nature (London)* **438**, 197 (2005).
- <sup>19</sup>M. Breitholtz, T. Kihlgren, S. A. Lindgren, and L. Wallden, *Phys. Rev. B* **67**, 235416 (2003).
- <sup>20</sup>M. Breitholtz, T. Kihlgren, S. Å. Lindgren, H. Olin, E. Wahlström, and L. Walldén, *Phys. Rev. B* **64**, 073301 (2001).
- <sup>21</sup>S. Kim, J. Ihm, H. J. Choi, and Y.-W. Son, *Phys. Rev. Lett.* **100**, 176802 (2008).
- <sup>22</sup>A. Bostwick, T. Ohta, T. Seyller, K. Horn, and E. Rotenberg, *Nat. Phys.* **3**, 36 (2007).
- <sup>23</sup>P. L. McEuen, M. Bockrath, D. H. Cobden, Y.-G. Yoon, and S. G. Louie, *Phys. Rev. Lett.* **83**, 5098 (1999).
- <sup>24</sup>J. R. Ahn, G. J. Yoo, J. T. Seo, J. H. Byun, and H. W. Yeom, *Phys. Rev. B* **72**, 113309 (2005).
- <sup>25</sup>C.-H. Park, F. Giustino, J. L. McChesney, A. Bostwick, T. Ohta, E. Rotenberg, M. L. Cohen, and S. G. Louie, *Phys. Rev. B* **77**, 113410 (2008).